ACS OMEGA

Open Access

http://pubs.acs.org/journal/acsodf

Article

Dual Mode Analysis of Methicillin-Resistant *Staphylococcus aureus* by the CRISPR/Cas12a-Assisted Exonuclease-Mediated Signal Cycle

Jing Xu, Qiang Ma, and Ya'e Kang*

Cite This: *ACS Omega* 2025, 10, 17820−17826

Read Online

ACCESS | Metrics & More | Article Recommendations | Supporting Information

ABSTRACT: Methicillin-resistant *Staphylococcus aureus* (MRSA) is the main Gram-positive bacteria isolated from patients with ocular infections and remians a huge threat to public health. Therefore, sensitive and dual-mode analysis of MRSA is of great significance for evaluating MRSA infection. We depicted a clustered regularly interspaced short palindromic repeats (CRISPR)/Cas12a-based biosensor by integrating the exonuclease III (Exo III)-enhanced fluorescence and colorimetric signals for sensitive and dual-mode analysis of methicillin resistance in MRSA without needing nucleic acid amplification. In this method, Exo III-assisted signal recycling is triggered only when the target *mecA* gene activates the CRISPR/Cas12a complex, and the HP probes on the surface of magnetic nanoparticles are cleaved by the trans-cleavage activity of Cas12a. Taking the merits of the trans-cleavage activity of the CRISPR/Cas12a system and the Exo III-assisted signal recycling, this approach exhibits an exceptionally elevated detection threshold for the *mecA* gene. Besides MRSA detection, this accurate and sensitive sensor can be employed to assess additional biomarkers in disease diagnosis by simply changing the crRNA.

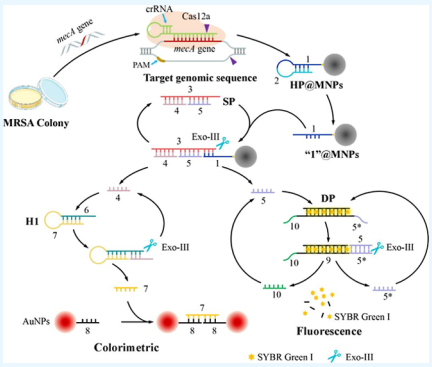

1. INTRODUCTION

Staphylococcus aureus accounts for one of the main Gram-positive bacteria isolated from patients with ocular infections.[1,2] Former research indicates that the *S. aureus* isolates are commonly resistant to multiple antibiotics; therefore, antibacterial susceptibility test results should be extensively considered in treating eye infections.[3−5] As one of the most prevalent and pervasive drug-resistant bacteria, MRSA is responsible for substantial morbidity and mortality.[6−8] MRSA strains have been widely observed in patients with eye infections, which poses a significant threat to the treatment. The rapid and precise identification of MRSA is essential to prevent its detrimental effects and monitor its spread within a population. Currently, MRSA detection is achieved through the use of colony culture-based antimicrobial susceptibility tests,[9−11] nucleic acid amplification tests,[12−14] and aptamer-based techniques.[15−18] However, these strategies typically necessitate a lengthy identification period and costly apparatus. Consequently, it is imperative to develop rapid, cost-effective, and sensitive biosensors to detect MRSA in ocular infections.

The clustered regularly interspaced short palindromic repeats (CRISPR)/associated nuclease 12a (CRISPR/Cas12a) system is a class 2 type V-A adaptive immunity that has been extensively used in the construction of biosensors and gene editing since its accurate target recognition capability and collateral trans-cleavage activity on surrounding single-stranded DNA (ssDNA) were reported.[19,20] The CRISPR/Cas12a-based biosensor has been employed to detect nucleic acids,[21,22] metal ions,[23] and exosomes.[24] Nevertheless, the CRISPR/Cas12a method alone has a detection limit of 0.1 nM for DNA, which is insufficient to detect the target at a low level.[25] To enhance the detection sensitivity, the CRISPR/Cas12a system was equipped with certain nucleic acid amplification techniques, including recombinant polymerase amplification[26,27] and polymerase chain reaction.[28] However, the requirement of complicated primers and multiple enzymes unavoidably results in the transfer of contaminants from one sample to another, which ultimately leads to false-positive results. Therefore, nucleic acid amplification-free strategies with comparable sensitivities will become a new trend in CRISPR/Cas12a-based detection.

Exonuclease III (Exo III)-assisted target recycling has gained increasing interest recently because of its notable sensitivity, simple design, and convenient operation.[29−31] Exo III is an enzyme that is more advanced than a nicking endonuclease and is commonly used in target recycling to detect specific DNA sequences.[32] Unlike a nicking endonuclease, Exo III does not require a specific recognition site and can work with various target sequences, making it suitable for creating

Received: January 17, 2025
Revised: April 15, 2025
Accepted: April 16, 2025
Published: April 24, 2025

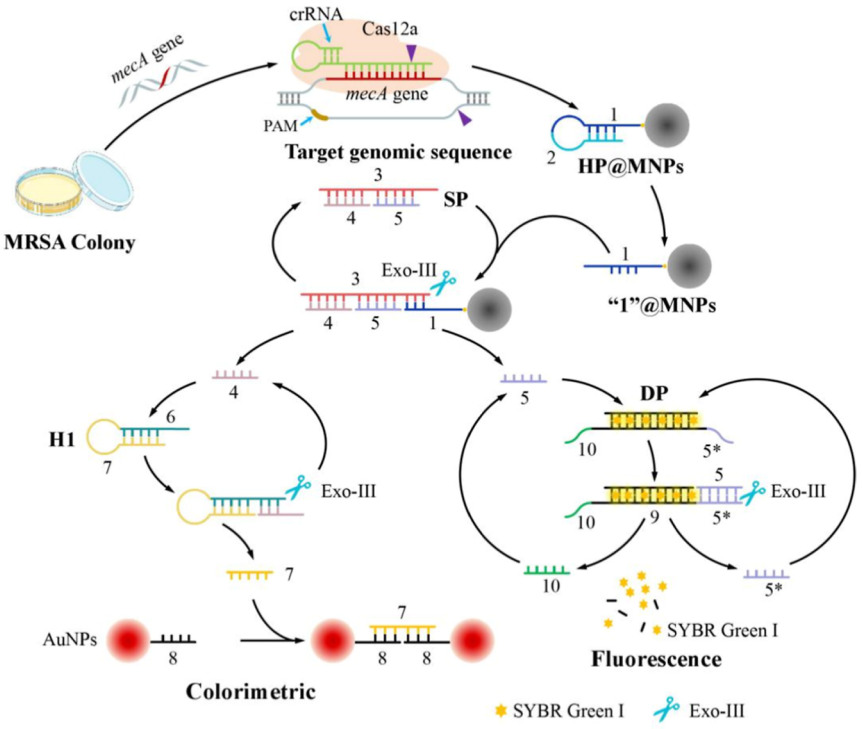

Figure 1. Working mechanism of the proposed method for sensitive and dual-mode MRSA detection.

versatile detection platforms using colorimetric,[33] electrochemical,[34] and fluorescence methods.[35,36] In contrast to a single-signal mode, a dual-mode sensor offers critical advantages because it concentrates on the significant enhancement of the resolving power, accuracy, and repeatability of analytical measurements through the integration of two distinct sensors and the subsequent analysis of data or data patterns using appropriate statistical models. For example, the colorimetric assay could be applied for MRSA detection in resource-limited settings because the results can be read directly by the naked eye without the requirement of the fluorescence spectrophotometer to read the signals, and the fluorescence assay can provide quantitative analysis of MRSA under the assistance of a fluorescence spectrophotometer. Therefore, dual-mode analysis of MRSA by a colorimetric assay and fluorescence assay is versatile for various settings. Numerous endeavors have been undertaken to develop innovative sensors that are promising and rely on a dual-mode output to detect targets. Nevertheless, very few studies have documented the dual-mode detection of MRSA.

Here, we depict an innovative sensing strategy that integrates the CRISPR/Cas12a system-based accurate target recognition, Exo III-assisted signal cycle, and dual-mode signaling for sensitive and dual-mode MRSA detection, which enables the detection of MRSA without the need for nucleic acid amplification. The *mecA* gene, which mediates methicillin resistance of MRSA by coding for penicillin-binding protein 2a (a substitute for other PBPs in cross-linking of peptidoglycan chains), was detected by the proposed method. For the dual-mode signaling, gold nanoparticles (AuNPs) and SYBR Green I were employed to generate both the colorimetric and fluorescent signals. This ultrasensitive biosensor has the potential to be expanded to assay other resistant bacteria, thereby offering a promising arsenal for preventing their dissemination.

2. RESULTS AND DISCUSSION

2.1. Working Mechanism of the Proposed Method for MRSA Detection. The detection mechanism of the proposed method for *mecA* analysis is illustrated in Figure 1. Initially, the signal input involved the extraction of MRSA genomic DNA from a cell colony using a fast bacterial genomic DNA isolation kit. The proposed approach allowed for the direct detection of the isolated genomic sequences without further purification, hence facilitating rapid MRSA detection. The trans-cleavage activity of the CRISPR/Cas12a system was initiated upon identification of the *mecA* gene in the extracted genomic sequences. The hairpin structure probe (HP) probe, which is fixed to the surface of magnetic nanoparticles (MNPs), is composed of a DNA section ("2") and an RNA section ("1").

Upon activation of the trans-cleavage activity of the CRISPR/Cas12a system, the DNA section of the HP probe was cleaved, leaving the RNA section on MNPs ("1"@MNP). The double-stranded sensing probe (SP) is a dsDNA sequence that consists of three sequences: the "3," "4", and "5" sequences. The "5" sequence does not occupy the 3′ terminal (toehold) of the "3" sequence to prevent the possible fault-cleavage of the "3" sequence by the Exo III. The "1" sequence binds to the toehold section of the SP probe, forming a blunt 3′ terminal that can be recognized by the Exo III. Subsequently, Exo III cleaves the "3" sequence, releasing the "4" and "5" sequences for signal generation. In the color system, the "4" sequence attaches to the toehold of the H1 probe, creating a blunt terminal that can be detected by Exo III. Exo III then breaks down the "6" sequence, releasing the "4" sequence to initiate the next signal cycle. The sequence "7" initiates the aggregation of the AuNPs by facilitating the hybridization between the "8" sequence. The fluorescent system is constructed with a dsDNA probe (DP) that has two complementary toeholds ("5*" and "10") located at each end. The sequence "5" is bound with the sequence "5*" in DP to

https://doi.org/10.1021/acsomega.5c00503
ACS Omega 2025, 10, 17820−17826

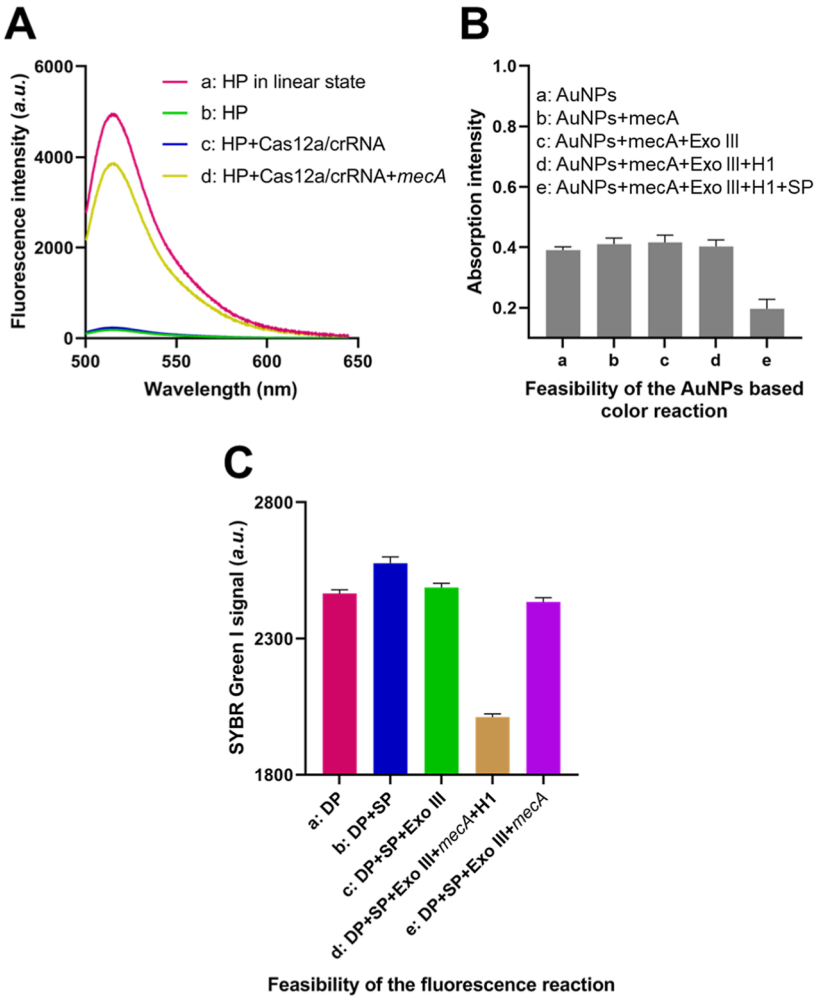

Figure 2. Feasibility of the sensing strategy. (A) Fluorescence spectrum of the FAM-labeled HP during the Cas12a/crRNA-mediated mecA recognition. (B) Absorbance peak of the color reaction when essential components existed or not. (C) SYBR Green I signals of the fluorescence reaction when essential components existed or not. Data were expressed as mean ± standard deviations, n = 3 technical duplicates. Data were expressed as mean ± standard deviations, n = 5 technical replicates.

create a blunt termination. The Exo III enzyme recognizes and cuts the specific sections labeled as "5*" and "9" in the lower sequence, resulting in the release of the "5" sequence, which then triggers the start of the next signal cycle. Additionally, the "10" sequence, which bears resemblance to the "5" sequence, can connect with DP and initiate signal recycling. Consequently, the double-stranded DNA (dsDNA) duplex sequences are broken down into single-stranded DNA (ssDNA) sequences, leading to a decrease in the signal of SYBR Green I.

2.2. Feasibility Analysis of the Strategy. The trans-cleavage activity of Cas12a, and the activation of CRISPR-Cas12a toward *mecA* was demonstrated. In this study, we conducted a fluorescent assay in which the two terminals of the HP probe were labeled with FAM and BHQ1. The fluorescence signal of HP tagged with FAM and BHQ1 was in low level (curve *b*) in comparison to that of the linear state (curve *a*) due to the proximity of FAM and BHQ1, as illustrated in Figure 2A. Meanwhile, the combination of Cas12a/crRNA and HP resulted in a faint signal (curve *c*), suggesting that the Cas12a/crRNA components had only a minimal impact on H1 stability. However, the addition of the *mecA* gene produced a robust fluorescence signal (curve d), demonstrating that the target-activated Cas12a/crRNA was capable of cleaving the DNA domain of H1, thereby leaving the entire RNA.

The viability of the dual-mode sensor for *mecA* detection was confirmed by studying the color changes and fluorescence intensity under various situations (Figure 2B). It was shown that in the reaction buffer solution, the surface plasmon absorption peak at 524 nm of the "8"@AuNPs was measured to be 0.3989 (column a). The stability of AuNPs was evidenced by the negligible alteration in absorption intensity (column b) following the introduction of the *mecA* gene into the system. Similarly, the recorded absorbance of AuNPs (column (c)) was not influenced by the inclusion of Exo III into the "8"@AuNPs system. This experiment demonstrated that Exo III did not have any effect on the color reaction of AuNPs. When "8"@AuNPs were exposed to the *mecA* gene, Exo III enzyme, and H1 probe, a noticeable alteration in the absorption intensity was seen in column e. The data indicated that the "4" sequence facilitated the color reaction.

The fluorescence measurement results are illustrated in Figure 2C. As anticipated, the DP exhibited a high fluorescence (column a), and this signal was slightly enhanced in the presence of SP (column b). Nevertheless, the fluorescence was diminished as a result of the specific digestion of SP by Exo III (column c) upon the introduction of the *mecA* gene.

https://doi.org/10.1021/acsomega.5c00503
ACS Omega 2025, 10, 17820−17826

Nevertheless, the fluorescence amplification was significantly reduced when the *mecA* gene, H1 probe, and Exo III were present in the same column (column d). The results presented above indicated that the dual-mode sensor was capable of detecting *mecA* in MRSA.

2.3. Analytical Performance of the Approach. The sensitivity of the CRISPR/Cas12a-based biosensor was systematically evaluated through colorimetric analysis. As shown in Figure 3A, a distinct color transition from pink to gray was observed in the "8"@AuNPs solution, corresponding to increasing concentrations of the *mecA* gene. Quantitative analysis revealed a progressive increase in the absorption intensity ratio (A_{620}/A_{520}) with *mecA* concentrations ranging from 0 to 10 nM (Figure 3B). Notably, the A_{620}/A_{520} ratio demonstrated an excellent linear relationship (R^2 = 0.9921) with *mecA* concentrations spanning from 10 fM to 100 pM (Figure 3B, inserted). The calibration curve was established using the following regression equation: $Y = 0.1432 \times \lg C + 0.1796$, where Y represents the A_{620}/A_{520} ratio, and C denotes the *mecA* concentration. The biosensor achieved a remarkable detection limit of less than 4.3 fM.

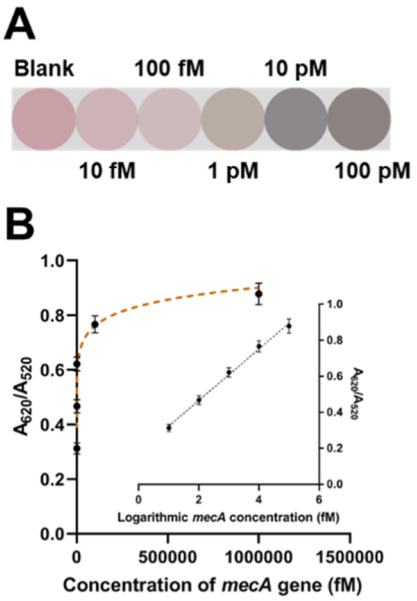

Figure 3. Colorimetric detection of the mecA gene. (A) Color changes of the method when detecting different concentrations of mecA. (B) A620/A520 ratio of the method when detecting different concentrations of mecA. Inserted is the linear correlation between the A620/A520 ratio and the logarithmic concentration of mecA. Data are expressed as mean ± standard deviations, n = 5 technical replicates.

A substantial increase in the difference in SYBR Green I intensity was observed as the concentration of the *mecA* gene increased within the 1 fM to 100 pM range for fluorescence analysis. The SYBR Green I signals in response to varying *mecA* gene concentrations are illustrated in Figure 4A. The calibration plots (Figure 4B) demonstrated a reasonable linear relationship between fluorescence intensity and *mecA* gene concentrations from 1 fM to 100 pM. Calibration equation (R^2 = 0.9902): $Y = 100.0 \times \lg C + 83.33$, where Y represents the difference in SYBR Green I intensity, and C represents the concentration of the *mecA* gene, was obtained. The *mecA* gene was detected using fluorescent sensing, which had a low LOD of 513 aM.

To assess the specificity of the *mecA* gene, control sequences including single-base mismatched *mecA* (mec-1), double-base mismatched *mecA* (mec-2), and triple-base mismatched *mecA* (mec-3) were selected for comparison. As demonstrated in Figure 5A,B, both the A_{620}/A_{520} ratio and fluorescence intensity values obtained from mec-1, mec-2, and mec-3 were significantly lower than those of the fully complementary *mecA* target gene. These results demonstrate that the developed method exhibits high accuracy and selectivity in *mecA* detection, which can be attributed to the precise target recognition capability of the CRISPR-Cas12a system combined with the exceptional ability of Exo III to distinguish single-base variations.[29,37] The CRISPR/Cas12a complex remains inactive until it specifically binds to the target DNA through complementary crRNA pairing.[22] This activation mechanism ensures that signal generation occurs exclusively when the CRISPR/Cas12a complex is triggered by the target DNA, leading to subsequent cleavage of the single-stranded DNA between the HP@MNPs.

2.4. Application of the Method for MRSA Detection. The sensitivity of the biosensor for MRSA detection, which is based on the CRISPR-Cas12a system, was evaluated by using

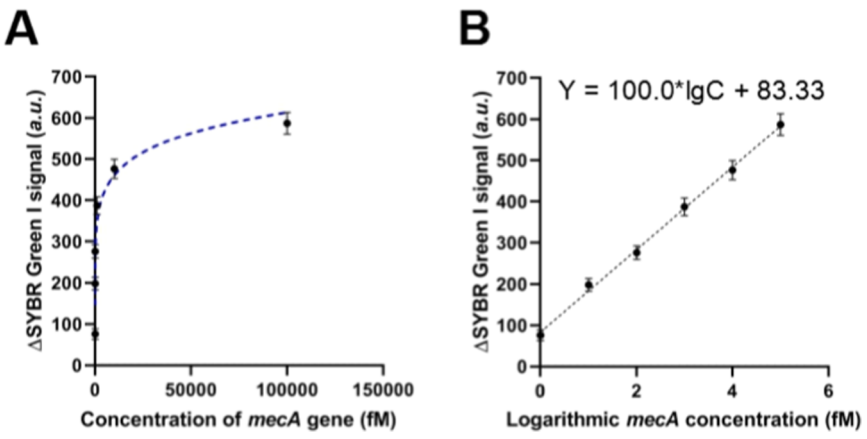

Figure 4. Fluorescence detection of the mecA gene. (A) SYBR Green I signals of the method when detecting different concentrations of mecA. (B) SYBR Green I signals of the method when detecting different concentrations of mecA. Data are expressed as mean ± standard deviations, n = 5 technical replicates.

https://doi.org/10.1021/acsomega.5c00503
ACS Omega 2025, 10, 17820−17826

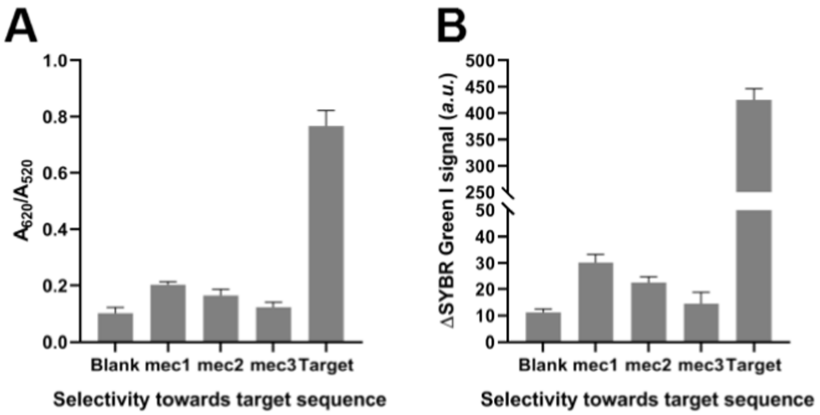

Figure 5. Selectivity of the method for mecA detection. (A) A_{620}/A_{520} ratio of the method when detecting interfering sequences and target sequences. (B) SYBR Green I signals of the method when detecting interfering sequences and target sequences. Data are expressed as mean ± standard deviations, n = 5 technical replicates.

optimal experimental conditions. For MRSA detection, the samples are prepared by diluting MRSA to different concentrations with commercial serum solutions to mimic clinical samples. The HP@AuNPs solution underwent a color transition from pink to gray, as depicted in Figure 6A,

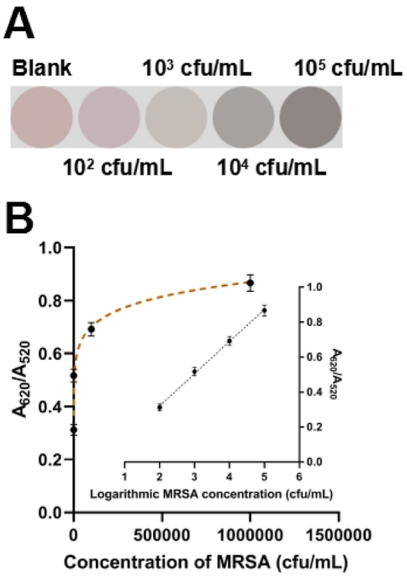

Figure 6. Colorimetric detection of the MRSA. (A) Color changes of the method when detecting different concentrations of MRSA. (B) A620/A520 ratio of the method when detecting different concentrations of MRSA. Data are expressed as mean ± standard deviations, n = 5 technical replicates.

indicating an increasing level of MRSA concentration. In addition, the absorption intensity ratio (A_{620}/A_{520}) increased gradually as the concentration of MRSA grew from 100 to 10^5 cfu/mL (Figure 6B). Moreover, there was a strong linear link between the absorption intensity ratio and the MRSA concentration, as shown in Figure 6B (inset). The calibration process was conducted using an equation of the following form: $Y = 0.1840 \times \lg C - 0.04700$. In this equation, Y represents the A_{620}/A_{520} ratio, and C represents the concentration of MRSA. The coefficient of determination (R^2) for this calibration equation is 0.9921. The colorimetric approach was shown to have a detection limit of 57 cfu/mL.

The fluorescence intensity increased significantly as the concentration of MRSA increased in the range of 10−10^6 cfu/mL for fluorescence analysis. Variations in intensity are illustrated in Figure 7A in response to varying MRSA concentrations. The calibration plots (Figure 7B) demonstrated a strong linear correlation between the logarithmic MRSA concentrations and fluorescence intensity. The calibration equation was $Y = 99.74 \times \lg C - 18.27$ (R^2 = 0.9886). Fluorescent sensing had a limit of detection of 4.1 cfu/mL for the detection of MRSA.

3. CONCLUSIONS

In conclusion, we have successfully developed a novel dual-mode detection system by integrating colorimetric and fluorescent signaling with the CRISPR/Cas12a platform, enabling the sensitive, specific, and reliable detection of the *mecA* gene. This innovative approach capitalizes on two key advantages: (i) the dual-signal output system, which significantly enhances detection accuracy by minimizing external interference through mutual signal verification, and (ii) the exceptional selectivity achieved through the synergistic combination of the precise target recognition capability of CRISPR-Cas12a and the base discrimination capability of Exo III. The system demonstrated excellent performance in *mecA* gene and MRSA detection, exhibiting a strong linear correlation (R^2 > 0.99) between fluorescence intensity and MRSA concentration. Comparative analysis with conventional methods revealed superior sensitivity and specificity (Table S2).[17,27] These findings suggest that our dual-mode detection strategy represents a significant advancement over existing methodologies, offering improved reliability for complex real-world applications requiring high precision. The successful implementation of this dual-mode sensor for *mecA* detection in MRSA not only validates its clinical applicability but also establishes a robust platform for biomarker quantification. This technological advancement opens new avenues for molecular diagnostics and biological research, particularly in the development of versatile testing devices for antimicrobial resistance detection (*Pseudomonas aeruginosa*) by simply changing the crRNA. Future studies should focus on expanding the application of the method to other clinically relevant biomarkers and optimizing its performance for field-deployable diagnostic platforms.

https://doi.org/10.1021/acsomega.5c00503
ACS Omega 2025, 10, 17820−17826

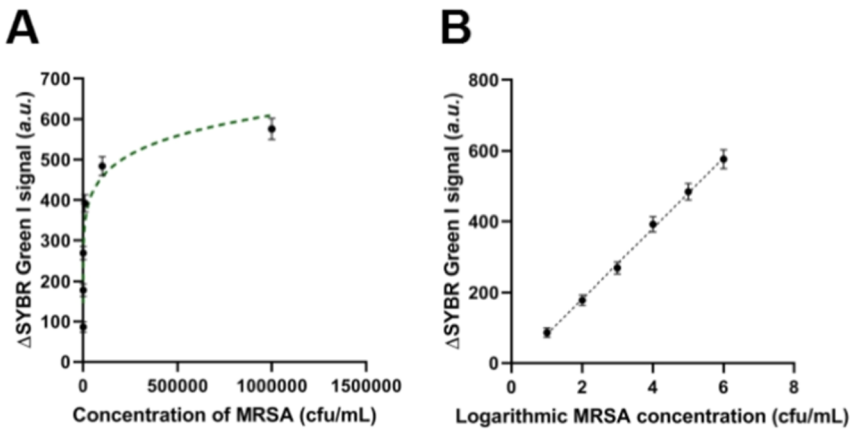

Figure 7. Fluorescence detection of the MRSA. (A) SYBR Green I signal changes in the method when detecting different concentrations of MRSA. (B) SYBR Green I signal changes in the method when detecting different concentrations of MRSA. Data are expressed as mean ± standard deviations, n = 5 technical replicates.

4. EXPERIMENTAL SECTION

4.1. Materials and Reagents. The sequences utilized in this study are designed according to former refs 38 and 39 The details of these sequences enumerated in Table S1 were acquired from Sangon Biotech Co., Ltd. (Shanghai, China). The Cas12a enzyme was acquired from New England Biolabs (Ipswich, MA, USA). The enzyme exonuclease III (Exo III) was acquired from TaKaRa Biotechnology Co., Ltd. (Dalian, China). The AuNPs were acquired from SANSURE Biotech Inc. (Changsha, China).

4.2. Feasibility Analysis of the Target-Mediated CRISPR-Cas12a Reaction. To verify the ability of the Cas12a enzyme to detect the *mecA* sequence, a mixture was prepared including 10 μL of generated *mecA* sequences, 10 μL of Cas12a enzyme, and FAM-tagged HP@MNPs. The mixture was kept at room temperature for 30 min, and the fluorescence signals were documented.

4.3. *mecA* Detection Using Fluorescence Measurements. The solution containing 10 μL of the Cas12a enzyme and HP@MNPs was supplemented with *mecA* at varying concentrations. The mixture was incubated at ambient temperature for 30 min, and then magnet-based enrichment of MNPs was performed. The Cas12a protein was deactivated by heating the mixture to 80 °C for 10 min. The liquid supernatant was subsequently combined with 10 μL of Exo III, 10 μL of SP, 10 μL of DP, and 10 μL of "8"@AuNPs. Finally, the fluorescence spectra were acquired using a Hitachi F-7000 fluorescence spectrometer (Tokyo, Japan).

4.4. Statistical Analysis. All quantitative data were expressed as mean ± standard deviation for normally distributed variables. The two-tailed Student's t-test was used to compare differences between two groups. All tests were two-tailed, with $p < 0.05$ considered statistically significant.

■ ASSOCIATED CONTENT

Data Availability Statement

Availability of data and materials: All experimental data are presented in the article or additional file.

Supporting Information

The Supporting Information is available free of charge at https://pubs.acs.org/doi/10.1021/acsomega.5c00503.

Sequences of the oligonucleotides used in the present study and brief comparisons of the method with former ones (PDF)

■ AUTHOR INFORMATION

Corresponding Author

Ya'e Kang − *Ophthalmology and Otorhinolaryngology Department, Shenmu City Hospital (Shenmu Hospital Affiliated to Northwest University), Yulin City 719300 Shaanxi Province, China;* orcid.org/0009-0001-7594-3420; Phone: 86-18091220275; Email: 18991319741@163.com

Authors

Jing Xu − *Department of Ophthalmology, First Affiliated Hospital of Northwestern University, Xi'an City 710016 Shaanxi Province, China*

Qiang Ma − *Department of Ophthalmology, First Affiliated Hospital of Northwestern University, Xi'an City 710016 Shaanxi Province, China*

Complete contact information is available at: https://pubs.acs.org/10.1021/acsomega.5c00503

Author Contributions

Y.K.: conceptualization, supervision, data curation, funding acquisition, and reviewing and editing the draft. **J.X.**: software, investigation, methodology, and writing an original draft. **Q.M.**: methodology and formal analysis.

Notes

The authors declare no competing financial interest.

■ REFERENCES

(1) McGuire, E.; Boyd, A.; Woods, K. Staphylococcus aureus Bacteremia. *Clin. Infect. Dis.* **2020**, *71* (10), 2765−2766.

(2) Oliveira, W. F.; Silva, P. M. S.; Silva, R. C. S.; Silva, G. M. M.; Machado, G.; Coelho, L.; Correia, M. T. S. Staphylococcus aureus and Staphylococcus epidermidis infections on implants. *J. Hosp. Infect.* **2018**, *98* (2), 111−117.

(3) Craft, K. M.; Nguyen, J. M.; Berg, L. J.; Townsend, S. D. Methicillin-resistant Staphylococcus aureus (MRSA): antibiotic-resistance and the biofilm phenotype. *Medchemcomm* **2019**, *10* (8), 1231−1241.

(4) Nandhini, P.; Kumar, P.; Mickymaray, S.; Alothaim, A. S.; Somasundaram, J.; Rajan, M. Recent Developments in Methicillin-

Resistant Staphylococcus aureus (MRSA) Treatment: A Review. *Antibiotics* **2022**, *11* (5), 606.
(5) Harford, D. A.; Greenan, E.; Knowles, S. J.; Fitzgerald, S.; Murphy, C. C. The burden of methicillin-resistant Staphylococcus aureus in the delivery of eye care. *Eye* **2022**, *36* (7), 1368−1372.
(6) Miao, J.; Chen, L.; Wang, J.; Wang, W.; Chen, D.; Li, L.; Li, B.; Deng, Y.; Xu, Z. Current methodologies on genotyping for nosocomial pathogen methicillin-resistant Staphylococcus aureus (MRSA). *Microb. Pathog.* **2017**, *107*, 17−28.
(7) Giuffre, M.; Bonura, C.; Cipolla, D.; Mammina, C. MRSA infection in the neonatal intensive care unit. *Expert Rev. Anti-Infect. Ther.* **2013**, *11* (5), 499−509.
(8) Reygaert, W. Methicillin-resistant Staphylococcus aureus (MRSA): identification and susceptibility testing techniques. *Clin. Lab. Sci.* **2009**, *22* (2), 120−124.
(9) Wang, J. C.; Tung, Y. C.; Ichiki, K.; Sakamoto, H.; Yang, T. H.; Suye, S. I.; Chuang, H. S. Culture-free detection of methicillin-resistant Staphylococcus aureus by using self-driving diffusometric DNA nanosensors. *Biosens. Bioelectron.* **2020**, *148*, 111817.
(10) Rich, M.; Jones, M.; Roberts, L. Enrichment culture for the detection of MRSA in companion animals. *Vet. Rec.* **2007**, *160* (8), 275.
(11) Zheng, L.; Shen, Y.; Dong, W.; Zheng, C.; Zhou, R.; Lou, Y. L. Rapid Detection and Antimicrobial Susceptibility Testing of Pathogens Using AgNPs-Invertase Complexes and the Personal Glucose Meter. *Front. bioeng. biotechnol.* **2022**, *9*, 795415.
(12) Alarcon, B.; Vicedo, B.; Aznar, R. PCR-based procedures for detection and quantification of Staphylococcus aureus and their application in food. *J. Appl. Microbiol.* **2006**, *100* (2), 352−364.
(13) Olcu, M.; Atalay, M. A.; Percin Renders, D. Development of multiplex PCR panel for detection of anaerobic bacteria in clinical samples. *Anaerobe* **2022**, *76*, 102611.
(14) Pan, J.; Bao, D.; Bao, E.; Chen, J. A hairpin probe-mediated DNA circuit for the detection of the mecA gene of Staphylococcus aureus based on exonuclease III and DNAzyme-mediated signal amplification. *Analyst* **2021**, *146* (11), 3673−3678.
(15) Ota, Y.; Furuhashi, K.; Nanba, T.; Yamanaka, K.; Ishikawa, J.; Nagura, O.; Hamada, E.; Maekawa, M. A rapid and simple detection method for phenotypic antimicrobial resistance in Escherichia coli by loop-mediated isothermal amplification. *J. Med. Microbiol.* **2019**, *68* (2), 169−177.
(16) Wei, L.; Wang, Z.; Wang, J.; Wang, X.; Chen, Y. Aptamer-based colorimetric detection of methicillin-resistant Staphylococcus aureus by using a CRISPR/Cas12a system and recombinase polymerase amplification. *Anal. Chim. Acta* **2022**, *1230*, 340357.
(17) Xu, L.; Dai, Q.; Shi, Z.; Liu, X.; Gao, L.; Wang, Z.; Zhu, X.; Li, Z. Accurate MRSA identification through dual-functional aptamer and CRISPR-Cas12a assisted rolling circle amplification. *J. Microbiol. Methods* **2020**, *173*, 105917.
(18) Chen, W.; Lai, Q.; Zhang, Y.; Liu, Z. Recent Advances in Aptasensors For Rapid and Sensitive Detection of Staphylococcus Aureus. *Front. bioeng. biotechnol.* **2022**, *10*, 889431.
(19) Han, J.; Kim, S.; Kim, S.; Lee, E. S.; Cha, B. S.; Park, J. S.; Shin, J.; Jang, Y.; Park, K. S. Cas12a-based primer production enables isothermal amplification for nucleic acid detection. *Sens. Actuators, B* **2023**, *381*, 133401.
(20) Han, J.; Shin, J.; Lee, E. S.; Cha, B. S.; Kim, S.; Jang, Y.; Kim, S.; Park, K. S. Cas12a/blocker DNA-based multiplex nucleic acid detection system for diagnosis of high-risk human papillomavirus infection. *Biosens. Bioelectron.* **2023**, *232*, 115323.
(21) Wang, R.; Zhao, X.; Chen, X.; Qiu, X.; Qing, G.; Zhang, H.; Zhang, L.; Hu, X.; He, Z.; Zhong, D.; Wang, Y.; Luo, Y. Rolling Circular Amplification (RCA)-Assisted CRISPR/Cas9 Cleavage (RACE) for Highly Specific Detection of Multiple Extracellular Vesicle MicroRNAs. *Anal. Chem.* **2020**, *92* (2), 2176−2185.
(22) Zhang, G. Z. L.; Zhang, L.; Tong, J.; Zhao, X.; Ren, J. CRISPR-Cas12a enhanced rolling circle amplification method for ultrasensitive miRNA detection. *Microchem. J.* **2020**, *158* (2020), 105239.
(23) Chen, Y.; Wu, H.; Qian, S.; Yu, X.; Chen, H.; Wu, J. Applying CRISPR/Cas system as a signal enhancer for DNAzyme-based lead ion detection. *Anal. Chim. Acta* **2022**, *1192*, 339356.
(24) Zhao, X.; Zeng, L.; Mei, Q.; Luo, Y. Allosteric Probe-Initiated Wash-Free Method for Sensitive Extracellular Vesicle Detection through Dual Cycle-Assisted CRISPR-Cas12a. *ACS Sens.* **2020**, *5* (7), 2239−2246.
(25) Zhao, X.; Tian, X.; Wang, Y.; Li, L.; Yu, Y.; Zhao, S.; Zhang, J. CRISPR-Cas12a-activated palindrome-catalytic hairpin assembly for ultrasensitive fluorescence detection of HIV-1 DNA. *Anal. Chim. Acta* **2022**, *1227*, 340303.
(26) Sun, Y.; Yu, L.; Liu, C.; Ye, S.; Chen, W.; Li, D.; Huang, W. One-tube SARS-CoV-2 detection platform based on RT-RPA and CRISPR/Cas12a. *J. Transl. Med.* **2021**, *19* (1), 74.
(27) Liu, Y.; Liu, H.; Yu, G.; Sun, W.; Aizaz, M.; Yang, G.; Chen, L. One-tube RPA-CRISPR Cas12a/Cas13a rapid detection of methicillin-resistant Staphylococcus aureus. *Anal. Chim. Acta* **2023**, *1278*, 341757.
(28) Fueller, J.; Herbst, K.; Meurer, M.; Gubicza, K.; Kurtulmus, B.; Knopf, J. D.; Kirrmaier, D.; Buchmuller, B. C.; Pereira, G.; Lemberg, M. K.; Knop, M. CRISPR-Cas12a-assisted PCR tagging of mammalian genes. *J. Cell Biol.* **2020**, *219* (6), No. e201910210.
(29) Zhou, Y.; Yu, S.; Shang, J.; Chen, Y.; Wang, Q.; Liu, X.; Wang, F. Construction of an Exonuclease III-Propelled Integrated DNAzyme Amplifier for Highly Efficient microRNA Detection and Intracellular Imaging with Ultralow Background. *Anal. Chem.* **2020**, *92* (22), 15069−15078.
(30) Xu, G.; Liu, X.; Shao, K.; Yu, X.; Hu, X.; Zhao, X.; Gong, Z. Universal platform for accurately damage-free mapping of sEVs cargo information. *Anal. Chim. Acta* **2022**, *1232*, 340432.
(31) Zhao, X.; Yuan, Y.; Liu, X.; Mao, F.; Xu, G.; Liu, Q. A Versatile Platform for Sensitive and Label-Free Identification of Biomarkers through an Exo-III-Assisted Cascade Signal Amplification Strategy. *Anal. Chem.* **2022**, *94* (4), 2298−2304.
(32) Liu, S.; Yu, X.; Wang, J.; Liu, D.; Wang, L.; Liu, S. Exonuclease III-Powered Self-Propelled DNA Machine for Distinctly Amplified Detection of Nucleic Acid and Protein. *Anal. Chem.* **2020**, *92* (14), 9764−9771.
(33) Xu, L.; Shen, X.; Li, B.; Zhu, C.; Zhou, X. G-quadruplex based Exo III-assisted signal amplification aptasensor for the colorimetric detection of adenosine. *Anal. Chim. Acta* **2017**, *980*, 58−64.
(34) Feng, C.; Zhang, C.; Guo, J.; Li, G.; Ye, B.; Zou, L. Novel electrochemical biosensor based on Exo III-assisted digestion of dsDNA polymer from hybridization chain reaction in homogeneous solution for CYFRA 21−1 DNA assay. *Anal. Chim. Acta* **2021**, *1158*, 338413.
(35) Guo, J.; Liang, Q.; Zhang, H.; Tian, M.; Zhang, H.; Wei, G.; Zhang, W. Exo-III Enzyme-Assisted Triple Cycle Signal Amplifications for Sensitive and Accurate Identification of Pathogenic Bacteria. *Appl. Biochem. Biotechnol.* **2023**, *195*, 6203−6211.
(36) Qu, X.; Zhu, D.; Yao, G.; Su, S.; Chao, J.; Liu, H.; Zuo, X.; Wang, L.; Shi, J.; Wang, L.; Huang, W.; Pei, H.; Fan, C. An Exonuclease III-Powered, On-Particle Stochastic DNA Walker. *Angew. Chem., Int. Ed. Engl.* **2017**, *56* (7), 1855−1858.
(37) Yang, Y.; Liu, J.; Zhou, X. A CRISPR-based and post-amplification coupled SARS-CoV-2 detection with a portable evanescent wave biosensor. *Biosens. Bioelectron.* **2021**, *190*, 113418.
(38) Fan, X.; Gao, Z.; Ling, D.; Wang, D.; Cui, Y.; Du, H.; Zhou, X. The dCas9/crRNA linked immunological assay (dCLISA) for sensitive, accurate, and facile drug resistance gene analysis. *Biosens. Bioelectron.* **2025**, *273*, 117147.
(39) Zhao, C.; Yang, Z.; Hu, T.; Liu, J.; Zhao, Y.; Leng, D.; Yang, K.; An, G. CRISPR-Cas12a based target recognition initiated duplex-specific nuclease enhanced fluorescence and colorimetric analysis of cell-free DNA (cfDNA). *Talanta* **2024**, *271*, 125717.

https://doi.org/10.1021/acsomega.5c00503
ACS Omega 2025, 10, 17820−17826